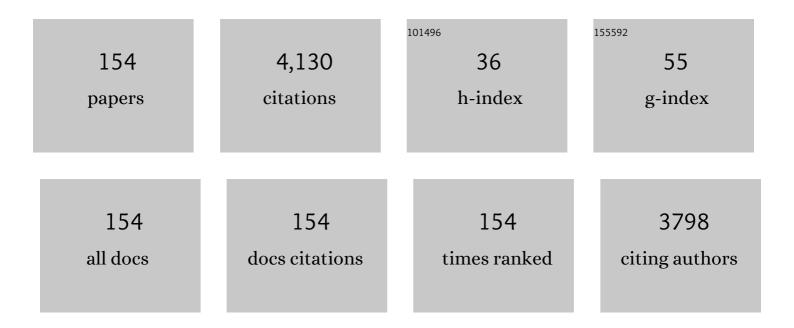
Jianping Wang

List of Publications by Year in descending order

Source: https://exaly.com/author-pdf/1018435/publications.pdf Version: 2024-02-01



LIANDING WANG

#	Article	IF	CITATIONS
1	Fibromodulin is involved in autophagy and apoptosis of granulosa cells affecting the follicular atresia in chicken. Poultry Science, 2022, 101, 101524.	1.5	11
2	miR-23b-3p inhibits chicken granulosa cell proliferation and steroid hormone synthesis via targeting GDF9. Theriogenology, 2022, 177, 84-93.	0.9	19
3	Filamin C regulates skeletal muscle atrophy by stabilizing dishevelled-2 to inhibit autophagy and mitophagy. Molecular Therapy - Nucleic Acids, 2022, 27, 147-164.	2.3	8
4	Alleviating effect of dietary supplementation of benzoic acid, Enterococcus faecium and essential oil complex on coccidia and Clostridium perfringens challenge in laying hens. Poultry Science, 2022, 101, 101720.	1.5	6
5	(C16H28N)2SbCl5: A new lead-free zero-dimensional metal-halide hybrid with bright orange emission. Science China Materials, 2022, 65, 1594-1600.	3.5	53
6	Limits in enhancement factor in near-brewster angle reflection pump-probe two-dimensional infrared spectroscopy. Chinese Journal of Chemical Physics, 2022, 35, 129-142.	0.6	0
7	Pure White Emission with 91.9% Photoluminescence Quantum Yield of [(C ₃ H ₇) ₄ N] ₂ Cu ₂ I ₄ out of Polaronic States and Ultra-High Color Rendering Index. ACS Applied Materials & Interfaces, 2022, 14. 12395-12403.	4.0	47
8	Dietary resveratrol improved production performance, egg quality, and intestinal health of laying hens under oxidative stress. Poultry Science, 2022, 101, 101886.	1.5	10
9	Conformation and Metal Cation Binding of Zwitterionic Alanine Tripeptide in Saline Solutions by Infrared Vibrational Spectroscopy and Molecular Dynamics Simulations. Journal of Physical Chemistry B, 2022, 126, 161-173.	1.2	2
10	Highly Efficient Broadband Green Emission of (TPA)CuCl ₂ Single Crystals: Understanding the Formation of Self-Trapped States. Journal of Physical Chemistry C, 2022, 126, 8545-8552.	1.5	18
11	Effect of benzoic acid on production performance, egg quality, intestinal morphology, and cecal microbial community of laying hens. Poultry Science, 2021, 100, 196-205.	1.5	24
12	Bulk assembly of a 0D organic antimony chloride hybrid with highly efficient orange dual emission by self-trapped states. Journal of Materials Chemistry C, 2021, 9, 12184-12190.	2.7	43
13	Bulk assembly of a OD organic tin(<scp>ii</scp>)chloride hybrid with high anti-water stability. Chemical Communications, 2021, 57, 8162-8165.	2.2	21
14	Dielectric polarization effect and transient relaxation in FAPbBr ₃ films before and after PMMA passivation. Physical Chemistry Chemical Physics, 2021, 23, 10153-10163.	1.3	14
15	Zearalenone Induces Apoptosis and Cytoprotective Autophagy in Chicken Granulosa Cells by PI3K-AKT-mTOR and MAPK Signaling Pathways. Toxins, 2021, 13, 199.	1.5	30
16	Highly Efficient Cool-White Photoluminescence of (Gua) ₃ Cu ₂ I ₅ Single Crystals: Formation and Optical Properties. ACS Applied Materials & Interfaces, 2021, 13, 13443-13451.	4.0	63
17	Dietary apple pectic oligosaccharide improves reproductive performance, antioxidant capacity, and ovary function of broiler breeders. Poultry Science, 2021, 100, 100976.	1.5	3
18	Water-Stable Zero-Dimensional (C ₄ H ₉) ₄ NCuCl ₂ Single Crystal with Highly Efficient Broadband Green Emission. Journal of Physical Chemistry Letters, 2021, 12, 6639-6647.	2.1	53

#	Article	IF	CITATIONS
19	Effect of 25-Hydroxycholecalciferol with Different Vitamin D3 Levels in the Hens Diet in the Rearing Period on Growth Performance, Bone Quality, Egg Production, and Eggshell Quality. Agriculture (Switzerland), 2021, 11, 698.	1.4	7
20	Dietary 25-hydroxyvitamin D improves intestinal health and microbiota of laying hens under high stocking density. Poultry Science, 2021, 100, 101132.	1.5	22
21	Organic Selenium Increased Gilts Antioxidant Capacity, Immune Function, and Changed Intestinal Microbiota. Frontiers in Microbiology, 2021, 12, 723190.	1.5	20
22	Bulk Assembly of Zero-Dimensional Organic Copper Bromide Hybrid with Bright Self-Trapped Exciton Emission and High Antiwater Stability. Journal of Physical Chemistry C, 2021, 125, 20014-20021.	1.5	33
23	Limitation and Potential Effects of Different Levels of Aging Corn on Performance, Antioxidative Capacity, Intestinal Health, and Microbiota in Broiler Chickens. Animals, 2021, 11, 2832.	1.0	2
24	Organic-inorganic hybrid manganese bromine single crystal with dual-band photoluminescence from polaronic and bipolaronic excitons. Nano Energy, 2021, 87, 106166.	8.2	85
25	Serum trimethylamine-N-oxide and gut microbiome alterations are associated with cholesterol deposition in the liver of laying hens fed with rapeseed meal. Animal Nutrition, 2021, 7, 1258-1270.	2.1	6
26	Dietary tributyrin improves reproductive performance, antioxidant capacity, and ovary function of broiler breeders. Poultry Science, 2021, 100, 101429.	1.5	14
27	Identifying genomic regions controlling ratoon stunting disease resistance in sugarcane (Saccharum) Tj ETQq1	1 0.78431 2.3	4 rgBT /Over
28	Dual self-trapped exciton emission of (TBA) ₂ Cu ₂ I ₄ : optical properties and high anti-water stability. Journal of Materials Chemistry C, 2021, 9, 16014-16021.	2.7	24
29	Ultrafast Structure and Vibrational Dynamics of a Cyano-Containing Non-Fullerene Acceptor for Organic Solar Cells Revealed by Two-Dimensional Infrared Spectroscopy. Journal of Physical Chemistry B, 2021, 125, 11987-11995.	1.2	2
30	Effect of organic acids on growth performance, intestinal morphology, and immunity of broiler chickens with and without coccidial challenge. AMB Express, 2021, 11, 140.	1.4	23
31	Effects of Dietary Iron on Manganese Utilization in Broilers Fed with Corn-Soybean Meal Diet. Biological Trace Element Research, 2020, 194, 514-524.	1.9	5
32	Dietary administration of resistant starch improved caecal barrier function by enhancing intestinal morphology and modulating microbiota composition in meat duck. British Journal of Nutrition, 2020, 123, 172-181.	1.2	24
33	Ultrafast Intermolecular Vibrational Energy Transfer in Hexahydro-1,3,5-trinitro-1,3,5-triazine in Molecular Crystal by 2D IR Spectroscopy. Journal of Physical Chemistry C, 2020, 124, 2388-2398.	1.5	11
34	Green tea polyphenol epigallocatechin-3-gallate improves the antioxidant capacity of eggs. Food and Function, 2020, 11, 534-543.	2.1	29
35	Proteomic alteration of albumen by dietary vanadium in commercial egg-type layers. Poultry Science, 2020, 99, 1705-1716.	1.5	2
36	Ultrafast Vibrational Energy Transfer through the Covalent Bond and Intra- and Intermolecular Hydrogen Bonds in a Supramolecular Dimer by Two-Dimensional Infrared Spectroscopy. Journal of Physical Chemistry B, 2020, 124, 544-555.	1.2	7

#	Article	IF	CITATIONS
37	Specific and non-specific interactions between metal cations and zwitterionic alanine tripeptide in saline solutions reported by the symmetric carboxylate stretching and amide-II vibrations. Physical Chemistry Chemical Physics, 2020, 22, 25042-25053.	1.3	3
38	Glucose activates the primordial follicle through the AMPK/mTOR signaling pathway. Clinical and Translational Medicine, 2020, 10, e122.	1.7	11
39	Excited-state photophysical processes in a molecular system containing perylene bisimide and zinc porphyrin chromophores. Physical Chemistry Chemical Physics, 2020, 22, 20891-20900.	1.3	5
40	Dietary supplementation of 25-hydroxycholecalciferol increases tibial mass by suppression bone resorption in meat ducks. Animal Nutrition, 2020, 6, 467-479.	2.1	6
41	Characterization of the Intestinal Microbiota of Broiler Breeders With Different Egg Laying Rate. Frontiers in Veterinary Science, 2020, 7, 599337.	0.9	6
42	Highly Efficient Self-Trapped Exciton Emission of a (MA) ₄ Cu ₂ Br ₆ Single Crystal. Journal of Physical Chemistry Letters, 2020, 11, 4703-4710.	2.1	138
43	Effect of dietary 25-hydroxycholecalciferol supplementation and high stocking density on performance, egg quality, and tibia quality in laying hens. Poultry Science, 2020, 99, 2608-2615.	1.5	31
44	Tandem mass tag-based quantitative proteomics analysis and gelling properties in egg albumen of laying hens feeding tea polyphenols. Poultry Science, 2020, 99, 430-440.	1.5	10
45	Evolution of the structure and properties of mechanochemically synthesized pyrrolidine incorporated manganese bromide powders. Journal of Materials Chemistry C, 2020, 8, 6488-6495.	2.7	49
46	Fecal bacteria and metabolite responses to dietary lysozyme in a sow model from late gestation until lactation. Scientific Reports, 2020, 10, 3210.	1.6	13
47	Effects of Dietary Iron Concentration on Manganese Utilization in Broilers Fed with Manganese-Lysine Chelate-Supplemented Diet. Biological Trace Element Research, 2020, 198, 231-242.	1.9	4
48	Impact of Dietary Manganese on Intestinal Barrier and Inflammatory Response in Broilers Challenged with Salmonella Typhimurium. Microorganisms, 2020, 8, 757.	1.6	19
49	Direct Observation of Surface Polarons in Capped CuInS2 Quantum Dots by Ultrafast Pump–Probe Spectroscopies. Journal of Physical Chemistry Letters, 2019, 10, 5297-5301.	2.1	15
50	Ultrafast Excited-State Intermolecular Proton Transfer in Indigo Oligomer. Journal of Physical Chemistry A, 2019, 123, 6463-6471.	1.1	13
51	Development of an Axiom Sugarcane100K SNP array for genetic map construction and QTL identification. Theoretical and Applied Genetics, 2019, 132, 2829-2845.	1.8	41
52	Alteration of the Antioxidant Capacity and Gut Microbiota under High Levels of Molybdenum and Green Tea Polyphenols in Laying Hens. Antioxidants, 2019, 8, 503.	2.2	27
53	Superstretchable Dynamic Polymer Networks. Advanced Materials, 2019, 31, e1904029.	11.1	75
54	Microbial Mechanistic Insights into the Role of Sweet Potato Vine on Improving Health in Chinese Meishan Gilt Model. Animals, 2019, 9, 632.	1.0	6

#	Article	IF	CITATIONS
55	Ultrafast intramolecular vibrational energy transfer in carbon nitride hydrocolloid examined by femtosecond two-dimensional infrared spectroscopy. Journal of Chemical Physics, 2019, 150, 194703.	1.2	4
56	The impact of dietary supplementation of different feed additives on performances of broiler breeders characterized by different egg-laying rate. Poultry Science, 2019, 98, 6091-6099.	1.5	20
57	Effect of Sweet Potato Vine on the Onset of Puberty and Follicle Development in Chinese Meishan Gilts. Animals, 2019, 9, 297.	1.0	5
58	Intensified C≡C Stretching Vibrator and Its Potential Role in Monitoring Ultrafast Energy Transfer in 2D Carbon Material by Nonlinear Vibrational Spectroscopy. Journal of Physical Chemistry Letters, 2019, 10, 1402-1410.	2.1	8
59	Heterogeneous ice nucleation correlates with bulk-like interfacial water. Science Advances, 2019, 5, eaat9825.	4.7	60
60	Effects of commercial premix vitamin level on sternum growth, calcification and carcass traits in meat duck. Journal of Animal Physiology and Animal Nutrition, 2019, 103, 53-63.	1.0	6
61	Dietary phosphorus deficiency impaired growth, intestinal digestion and absorption function of meat ducks. Asian-Australasian Journal of Animal Sciences, 2019, 32, 1897-1906.	2.4	7
62	Methylation Mediated Anharmonic Vibrational Signature of Nucleobases: A Case Study of Uracil and Thymine. ChemistrySelect, 2018, 3, 4374-4381.	0.7	2
63	Efficient Intramolecular Vibrational Excitonic Energy Transfer in Ru ₃ (CO) ₁₂ Cluster Revealed by Two-Dimensional Infrared Spectroscopy. Journal of Physical Chemistry B, 2018, 122, 1296-1305.	1.2	15
64	Direct Anionic Effect on Water Structure and Indirect Anionic Effect on Peptide Backbone Hydration State Revealed by Thin-Layer Infrared Spectroscopy. Journal of Physical Chemistry B, 2018, 122, 68-76.	1.2	8
65	Central-metal effect on intramolecular vibrational energy transfer of M(CO) ₅ Br (M = Mn,) Tj ETQq1 1 3637-3647.	0.78431 1.3	4 rgBT /Ove 10
66	Solvent-dependent structural dynamics of an azido-platinum complex revealed by linear and nonlinear infrared spectroscopy. Physical Chemistry Chemical Physics, 2018, 20, 9984-9996.	1.3	8
67	Innovative method for creating fitted brassiere wire prototype based on transformation matrix algorithm. Journal of the Textile Institute, 2018, 109, 73-78.	1.0	5
68	Effect of graded calcium supplementation in low-nutrient density feed on tibia composition and bone turnover in meat ducks. British Journal of Nutrition, 2018, 120, 1217-1229.	1.2	11
69	Linear and Nonlinear Infrared Spectroscopies Reveal Detailed Solute–Solvent Dynamic Interactions of a Nitrosyl Ruthenium Complex in Solution. Journal of Physical Chemistry B, 2018, 122, 9225-9235.	1.2	7
70	Development and Applications of a High Throughput Genotyping Tool for Polyploid Crops: Single Nucleotide Polymorphism (SNP) Array. Frontiers in Plant Science, 2018, 9, 104.	1.7	89
71	Micellar and bicontinuous microemulsion structures show different solute–solvent interactions: a case study using ultrafast nonlinear infrared spectroscopy. Physical Chemistry Chemical Physics, 2018, 20, 19938-19949.	1.3	12
72	Integrated omics data of two annual ryegrass (Lolium multiflorum L.) genotypes reveals core metabolic processes under drought stress. BMC Plant Biology, 2018, 18, 26.	1.6	30

#	Article	IF	CITATIONS
73	EST-SSR marker characterization based on RNA-sequencing of Lolium multiflorum and cross transferability to related species. Molecular Breeding, 2018, 38, 1.	1.0	15
74	Construction of a prediction model for body dimensions used in garment pattern making based on anthropometric data learning. Journal of the Textile Institute, 2017, 108, 2107-2114.	1.0	40
75	Target enrichment sequencing in cultivated peanut (Arachis hypogaea L.) using probes designed from transcript sequences. Molecular Genetics and Genomics, 2017, 292, 955-965.	1.0	17
76	Ultrafast two-dimensional infrared spectroscopy for molecular structures and dynamics with expanding wavelength range and increasing sensitivities: from experimental and computational perspectives. International Reviews in Physical Chemistry, 2017, 36, 377-431.	0.9	32
77	A novel method for determining skin deformation of lower limb in cycling. Journal of the Textile Institute, 2017, 108, 1600-1608.	1.0	9
78	Vanadate oxidative and apoptotic effects are mediated by the MAPK-Nrf2 pathway in layer oviduct magnum epithelial cells. Metallomics, 2017, 9, 1562-1575.	1.0	37
79	Efficient Vibrational Energy Transfer through Covalent Bond in Indigo Carmine Revealed by Nonlinear IR Spectroscopy. Journal of Physical Chemistry B, 2017, 121, 9411-9421.	1.2	19
80	Vibrational Characterization of Two-Dimensional Graphdiyne Sheets. Journal of Physical Chemistry C, 2017, 121, 21430-21438.	1.5	16
81	Capturing the photoâ€signaling state of a photoreceptor in a steadyâ€state fashion by binding a transition metal complex. Protein Science, 2017, 26, 2249-2256.	3.1	Ο
82	Mining sequence variations in representative polyploid sugarcane germplasm accessions. BMC Genomics, 2017, 18, 594.	1.2	46
83	Different Types of Dietary Fibers Trigger Specific Alterations in Composition and Predicted Functions of Colonic Bacterial Communities in BALB/c Mice. Frontiers in Microbiology, 2017, 8, 966.	1.5	47
84	Comparative proteomic analyses reveal the proteome response to short-term drought in Italian ryegrass (Lolium multiflorum). PLoS ONE, 2017, 12, e0184289.	1.1	13
85	Transcriptional Profiles of Drought-Related Genes in Modulating Metabolic Processes and Antioxidant Defenses in Lolium multiflorum. Frontiers in Plant Science, 2016, 7, 519.	1.7	81
86	Natural Allelic Variations in Highly Polyploidy Saccharum Complex. Frontiers in Plant Science, 2016, 7, 804.	1.7	40
87	Differentiating Two Nitrosylruthenium Isomeric Complexes by Steady-State and Ultrafast Infrared Spectroscopies. Journal of Physical Chemistry B, 2016, 120, 11502-11509.	1.2	4
88	Effects of dietary nanocrystalline cellulose supplementation on growth performance, carcass traits, intestinal development and lipid metabolism of meat ducks. Animal Nutrition, 2016, 2, 192-197.	2.1	7
89	Uncovering the Sensitivity of Amide-II Vibration to Peptide–Ion Interactions. Journal of Physical Chemistry B, 2016, 120, 9590-9598.	1.2	20
90	Structural dynamics of nitrosylruthenium isomeric complexes studied with steady-state and transient pump-probe infrared spectroscopies. Spectrochimica Acta - Part A: Molecular and Biomolecular Spectroscopy, 2016, 166, 62-67.	2.0	1

#	Article	IF	CITATIONS
91	Two-Dimensional Infrared Study of ¹³ C-Natural Abundant Vibrational Transition Reveals Intramolecular Vibrational Redistribution Rather than Fluxional Exchange in Mn(CO) ₅ Br. Journal of Physical Chemistry B, 2016, 120, 1304-1311.	1.2	17
92	General Applicable Frequency Map for the Amide-I Mode in Î ² -Peptides. Journal of Physical Chemistry B, 2016, 120, 1069-1079.	1.2	16
93	Molecular marker development from transcript sequences and germplasm evaluation for cultivated peanut (Arachis hypogaea L.). Molecular Genetics and Genomics, 2016, 291, 363-381.	1.0	21
94	Structural dynamics ofN-ethylpropionamide clusters examined by nonlinear infrared spectroscopy. Journal of Chemical Physics, 2015, 143, 185102.	1.2	4
95	Ultrafast vibrational and structural dynamics of dimeric cyclopentadienyliron dicarbonyl examined by infrared spectroscopy. Physical Chemistry Chemical Physics, 2015, 17, 14542-14550.	1.3	13
96	Selectively Probing the Structures and Dynamics of β-Peptide Aggregates Using the Amide-A Vibrational Marker. Journal of Physical Chemistry B, 2015, 119, 15451-15459.	1.2	6
97	Understanding the Amide-II Vibrations in \hat{I}^2 -Peptides. Journal of Physical Chemistry B, 2015, 119, 14831-14839.	1.2	28
98	Dissecting Amide-I Vibration in β-Peptide Helices. Journal of Physical Chemistry B, 2015, 119, 3387-3397.	1.2	14
99	Structure and Dynamics of Ferrocyanide and Ferricyanide Anions in Water and Heavy Water: An Insight by MD Simulations and 2D IR Spectroscopy. Journal of Physical Chemistry B, 2014, 118, 14899-14912.	1.2	59
100	π onjugated Carbon Radicals at Graphene Oxide to Initiate Ultrastrong Chemiluminescence. Angewandte Chemie, 2014, 126, 10273-10277.	1.6	9
101	Photoisomerization and structural dynamics of two nitrosylruthenium complexes: a joint study by NMR and nonlinear IR spectroscopies. Physical Chemistry Chemical Physics, 2014, 16, 24045-24054.	1.3	11
102	Interaction between Metal Cation and Unnatural Peptide Backbone Mediated by Polarized Water Molecules: Study of Infrared Spectroscopy and Computations. Journal of Physical Chemistry B, 2014, 118, 12336-12347.	1.2	19
103	Hydration Dynamics of Cyanoferrate Anions Examined by Ultrafast Infrared Spectroscopy. Journal of Physical Chemistry B, 2014, 118, 3104-3114.	1.2	44
104	Amide-I Characteristics of Helical Î ² -Peptides by Linear Infrared Measurement and Computations. Journal of Physical Chemistry B, 2014, 118, 94-106.	1.2	21
105	Simultaneously Probing Two Ultrafast Condensedâ€Phase Molecular Symmetry Breaking Events by Twoâ€Dimensional Infrared Spectroscopy. ChemPhysChem, 2013, 14, 2497-2504.	1.0	11
106	Structural Dynamics of <i>N</i> -Propionyl- <scp>d</scp> -glucosamine Probed by Infrared Spectroscopies and Ab Initio Computations. Journal of Physical Chemistry A, 2013, 117, 6105-6115.	1.1	10
107	Chain-length and mode-delocalization dependent amide-I anharmonicity in peptide oligomers. Journal of Chemical Physics, 2012, 136, 214112.	1.2	17
108	Correlated High-Frequency Molecular Motions in Neat Liquid Probed with Ultrafast Overtone Two-Dimensional Infrared Spectroscopy. Journal of Physical Chemistry Letters, 2012, 3, 3665-3670.	2.1	23

#	Article	IF	CITATIONS
109	Spectroscopic Evidence for Polymorphic Aggregates Formed by Amyloidâ€Î² Fragments. ChemPhysChem, 2012, 13, 3901-3908.	1.0	14
110	Influence of an Unnatural Amino Acid Side Chain on the Conformational Dynamics of Peptides. ChemPhysChem, 2012, 13, 1522-1534.	1.0	10
111	Dynamical Structures of Glycol and Ethanedithiol Examined by Infrared Spectroscopy, Ab Initio Computation, and Molecular Dynamics Simulations. Journal of Physical Chemistry B, 2011, 115, 1175-1187.	1.2	8
112	Anharmonic overtone and combination states of glycine and two model peptides examined by vibrational self-consistent field theory. Physical Chemistry Chemical Physics, 2011, 13, 2001-2013.	1.3	13
113	Anharmonic vibrations of nucleobases: Structural basis of one- and two-dimensional infrared spectra for canonical and mismatched base pairs. Science China Chemistry, 2011, 54, 1590-1606.	4.2	3
114	Amide Vibrations and Their Conformational Dependences in β-Peptide. Journal of Physical Chemistry B, 2010, 114, 16011-16019.	1.2	11
115	Non-Native Side Chain IR Probe in Peptides: Ab Initio Computation and 1D and 2D IR Spectral Simulation. Journal of Physical Chemistry B, 2010, 114, 2327-2336.	1.2	14
116	Arene Control over Thiolate to Sulfinate Oxidation in Albumin by Organometallic Ruthenium Anticancer Complexes. Chemistry - A European Journal, 2009, 15, 6586-6594.	1.7	77
117	Ultrafast Structural Dynamics of Biomolecules Examined by Multipleâ€Mode 2D IR Spectroscopy: Anharmonically Coupled Motions are in Harmony. ChemPhysChem, 2009, 10, 2242-2250.	1.0	9
118	Conformational dependence of anharmonic NH stretch vibration in peptides. Chemical Physics Letters, 2009, 467, 375-380.	1.2	6
119	Structurally Sensitive Anharmonic C _α â^'D Stretch Vibration in Deuterated Peptides. Journal of Physical Chemistry B, 2009, 113, 1813-1816.	1.2	7
120	Rapid Thermal Tuning of Chromophore Structure in Membrane Protein. Journal of Physical Chemistry B, 2009, 113, 4184-4186.	1.2	1
121	Multiple Anharmonic Vibrational Probes of Sugar Structure and Dynamics. Journal of Physical Chemistry B, 2009, 113, 1681-1692.	1.2	11
122	Differentiating Subtle Variation of Weak Intramolecular Hydrogen Bond in Vicinal Diols by Linear Infrared Spectroscopy. Journal of Physical Chemistry A, 2009, 113, 6070-6076.	1.1	18
123	Assessment of the amide-I local modes in γ- and β-turns of peptides. Physical Chemistry Chemical Physics, 2009, 11, 5310.	1.3	28
124	Molecular mechanics force field-based map for peptide amide-I mode in solution and its application to alanine di- and tripeptides. Physical Chemistry Chemical Physics, 2009, 11, 9149.	1.3	34
125	Influence of Solvent Polarity and Hydrogen Bonding on the Electronic Transition of Coumarin 120: A TDDFT Study. ChemPhysChem, 2008, 9, 1593-1602.	1.0	42
126	Two-Dimensional Infrared Spectroscopy as a Probe of the Solvent Electrostatic Field for a Twelve Residue Peptide. Journal of Physical Chemistry B, 2008, 112, 5930-5937.	1.2	53

#	Article	IF	CITATIONS
127	Conformational Dependence of Anharmonic Vibrations in Peptides:  Amide-I Modes in Model Dipeptide. Journal of Physical Chemistry B, 2008, 112, 4790-4800.	1.2	36
128	Ab Initio-Based All-Mode Two-Dimensional Infrared Spectroscopy of a Sugar Molecule. Journal of Physical Chemistry B, 2007, 111, 9193-9196.	1.2	25
129	Photocurrent from Oriented Membrane Films Containing Acid-blue and Acid-purple Bacteriorhodopsin and its Mutants. Photochemistry and Photobiology, 2007, 71, 476-480.	1.3	0
130	The Effect of Metal Cation Binding on the Protein, Lipid and Retinal Isomeric Ratio in Regenerated Bacteriorhodopsin of Purple Membrane¶. Photochemistry and Photobiology, 2007, 73, 564-571.	1.3	0
131	Two-Dimensional Infrared Spectroscopy Displays Signatures of Structural Ordering in Peptide Aggregates. Biophysical Journal, 2006, 90, 4672-4685.	0.2	35
132	Local Structure of \hat{I}^2 -Hairpin Isotopomers by FTIR, 2D IR, and Ab Initio Theory. Journal of Physical Chemistry B, 2006, 110, 7545-7555.	1.2	119
133	Anharmonicity of Amide Modesâ€. Journal of Physical Chemistry B, 2006, 110, 3798-3807.	1.2	91
134	Coupling between C–D and CO motions using dual-frequency 2D IR photon echo spectroscopy. Chemical Physics Letters, 2006, 432, 122-127.	1.2	37
135	Two-Dimensional Infrared Spectroscopy of the Alanine Dipeptide in Aqueous Solution. Journal of Physical Chemistry B, 2005, 109, 7511-7521.	1.2	192
136	Characteristics of the two-dimensional infrared spectroscopy of helices from approximate simulations and analytic models. Chemical Physics, 2004, 297, 195-219.	0.9	91
137	Vibrational Coupling, Isotopic Editing, and β-Sheet Structure in a Membrane-Bound Polypeptide. Journal of the American Chemical Society, 2004, 126, 5843-5850.	6.6	111
138	The Assignment of the Different Infrared Continuum Absorbance Changes Observed in the 3000–1800-cmâ~'1 Region during the Bacteriorhodopsin Photocycle. Biophysical Journal, 2004, 87, 2676-2682.	0.2	51
139	Vibrational Coupling between Amide-I and Amide-A Modes Revealed by Femtosecond Two Color Infrared Spectroscopyâ€. Journal of Physical Chemistry A, 2003, 107, 3384-3396.	1.1	92
140	Dual-frequency 2D-IR spectroscopy heterodyned photon echo of the peptide bond. Proceedings of the National Academy of Sciences of the United States of America, 2003, 100, 5601-5606.	3.3	146
141	Refolding of Thermally Denatured Bacteriorhodopsin in Purple Membraneâ€. Journal of Physical Chemistry B, 2002, 106, 723-729.	1.2	15
142	Comparison of the Dynamics of the Primary Events of Bacteriorhodopsin in Its Trimeric and Monomeric States. Biophysical Journal, 2002, 83, 1557-1566.	0.2	54
143	Time-Resolved Long-Lived Infrared Emission from Bacteriorhodopsin during its Photocycle. Biophysical Journal, 2002, 83, 1589-1594.	0.2	8
144	Fourier Transform Infrared Study of the Effect of Different Cations on Bacteriorhodopsin Protein Thermal Stability. Biophysical Journal, 2002, 82, 1598-1606.	0.2	13

#	ARTICLE	IF	CITATIONS
145	Direct observation of charge-transfer dynamics in a conjugated conducting polymer poly(3-octylthiophene)-fullerene composite by time-resolved infrared spectroscopy. Physical Review B, 2001, 64, .	1.1	6
146	Time-Resolved Fourier Transform Infrared Spectroscopy of the Polarizable Proton Continua and the Proton Pump Mechanism of Bacteriorhodopsin. Biophysical Journal, 2001, 80, 961-971.	0.2	42
147	Temperature-Jump Investigations of the Kinetics of Hydrogel Nanoparticle Volume Phase Transitions. Journal of the American Chemical Society, 2001, 123, 11284-11289.	6.6	138
148	The Effect of Metal Cation Binding on the Protein, Lipid and Retinal Isomeric Ratio in Regenerated Bacteriorhodopsin of Purple Membrane¶. Photochemistry and Photobiology, 2001, 73, 564.	1.3	15
149	The Effect of Protein Conformation Change from αII to αI on the Bacteriorhodopsin Photocycle. Biophysical Journal, 2000, 78, 2031-2036.	0.2	39
150	Proton Polarizability of Hydrogen-Bonded Network and its Role in Proton Transfer in Bacteriorhodopsin. Journal of Physical Chemistry A, 2000, 104, 4333-4337.	1.1	11
151	Time-resolved Fourier-transform infrared and visible luminescence spectroscopy of photoexcited porous silicon. Physical Review B, 1999, 59, 5026-5031.	1.1	25
152	Temperature Jump-Induced Secondary Structural Change of the Membrane Protein Bacteriorhodopsin in the Premelting Temperature Region: A Nanosecond Time-Resolved Fourier Transform Infrared Study. Biophysical Journal, 1999, 76, 2777-2783.	0.2	57
153	Anharmonic Vibrational Signatures of Peptides $\hat{a} \in \mathbb{C}$ Methods and Applications. , 0, , .		0
154	Solution Structures and Ultrafast Vibrational Energy Dissipation Dynamics in Cyclotetramethylene Tetranitramine. Journal of Chemical Physics, 0, , .	1.2	1